February 4, 2004

Ken Zweibel
National Renewable Energy Laboratory
1617 Cole Boulevard
Golden, CO 80401

Re: NREL Subcontract #ADJ-1-30630-12

Dear Ken:

This report covers research conducted at the Institute of Energy Conversion (IEC) for the period Dec. 09, 2003 to Jan. 09, 2004, under the subject subcontract. The report highlights progress and results obtained under Task 2 ($CuInSe_2$-based Solar Cells).

## Task 2: $CuInSe_2$-based Solar Cells

### *In Line Evaporation System*

Previously, Upilex S web substrates that were tested in the in-line system following a Mo coating protocol where thick (low sheet resistance) Mo was deposited first on side 1, then thin Mo was deposited on side 2 of the 13" web. The deposition was performed at three different sputter pressures producing films under different stress states. After Mo coating was finished, the web was slit into two 6" wide rolls. These rolls had then both edges cut in the slitter. Deposition of $Cu(InGa)Se_2$ on all these rolls resulted in cracked and low adhesive CIGS-on-Mo films independent of the stress states.

On the basis of these observations it was decided to (1) deposit Mo on Upilex web pre-slit to 6" width and (2) deposit thin Mo first and thick Mo last. The idea was to minimize handling, especially of the thick Mo side, before depositing $Cu(InGa)Se_2$. However, when $Cu(InGa)Se_2$ was deposited on such substrates the resulting coating was found to have the largest amount of cracking so far observed, and the adhesion was very poor. At the present time, no explanation can be put forward for such dramatic changes in the behavior of the web metallized in different order.

During this period, improvements in the system hardware also continued. A new web shield with thermocouple holders attached to it has been put in place. These thermocouples are sheathed ungrounded K-type of 0.010" outside diameter and are positioned to touch the web's coating side by their natural "spring" action just before and just after the deposition zone. For heater platen temperatures of 500°C and 550°C respectively over the first half and the second half of the deposition zone, the respective web temperatures observed were around 400°C and 420°C. These thermocouples will eventually replace the thermocouples located in the heaters as the substrate control thermocouples.

A major reliability issue in the in-line system has been the operational life of the Cu source. After about ten to twenty runs, cracks develop on the BN internal boat at the thermocouple (TC) well causing liquid Cu leaking on the thermocouple. The boat and the TC have to be replaced, in order to avoid this problem, a new Cu source was designed that avoided sharp internal lines and corners as they invariably act as stress concentrators. The resulting boat, which also was designed to have larger capacity, has been put in service and operating reliably for some time now. Since, the issue of liquid Cu leaking into the TC well has been resolved, naked C type thermocouple, rather than a sheathed one is now being used.

In the new boat, however, a non-negligible difference between TC read-out and actual melt temperature was observed by monitoring solidification point during the cool-down. In order to quantify this "offset" and correct the set-point, before each run the Cu boat is heated and the load melting and cooling temperatures as a function of time, T(t), are recorded. In the first derivative, $dT/dt$ the phase transition shows up as a distinct peak, and in the second derivative, $d^2T/dt^2$, as a zero crossing. Figure 1 gives an example of such an analysis for run No. 70238. Taking the melting point of Cu as 1085°C, the analysis gives an offset of –167°C.

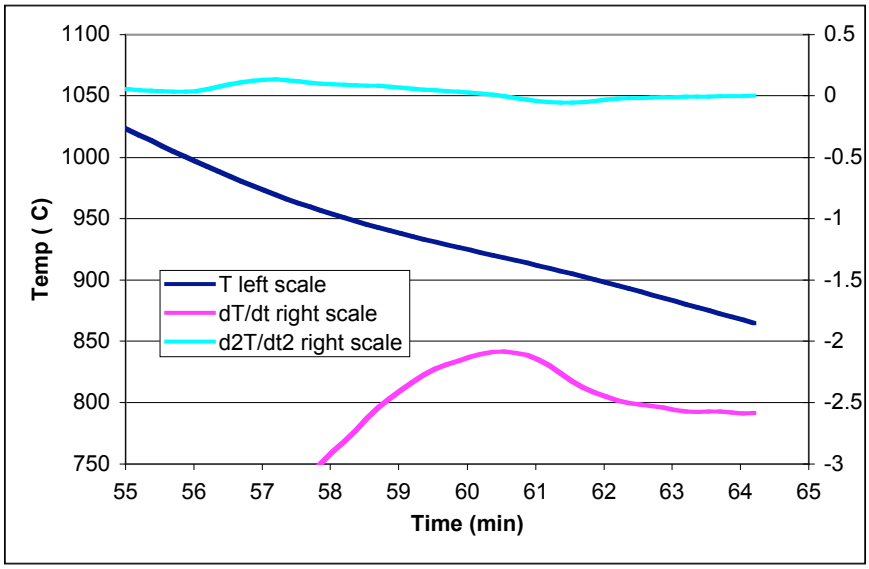


Figure 1. Determining the TC offset for the Cu source during run No. 70238.

## *Wide Bandgap Materials*

## S-diffusion in $Cu(InGa)Se_2$

The lattice diffusion coefficient $D_l$ governing the interdiffusion of Se and S in $CuInSe_2$ determined from AES depth profiles measured on sulfurized $CuInSe_2$ crystals was reported previously. Subsequent effort has focused on determining $D_l$ and the grain boundary diffusion coefficient $D_b$ independently from sulfurized $CuInSe_2$ films. This requires the preparation of very smooth films with well-defined columnar grains in order to allow for quantitative analysis of experimental depth profiles. Films prepared at IEC by co-evaporation have large grains but are too rough for a straight-forward experiment. Various approaches have been pursued in an effort to produce a sample that could be analyzed quantitatively.

The polishing procedure that had been used successfully in the preparation of crystals for sulfurization experiments cannot be applied to films because it would remove the entire film. Films were mechanically polished with alumina slurry then subjected to a mild chemical etch in KOH remove some damaged material to produce a mirror finish when the films were thinned from about 2 µm down to about 0.2 µm thickness. However, sulfurization of the films caused them to roughen up again so that no attempt at quantitative analysis was made. It is believed that the mechanical polish produced crystal defects in the remaining film, and that recrystallization of this damaged material resulted in a roughened film surface after sulfurization. Efforts to use a modified chemo-mechanical etch are underway.

Alternatively, films were pulled off their original substrate with electrically conductive high-temperature glue to leave a smooth exposed surface. After sulfurization, though, these films were also rough. It was found that they had intermixed with the underlying glue and had formed secondary phases.

In a third approach it is assumed that the value of $D_l$ obtained from crystals is also valid for films, so only $D_b$ needs to be determined. As-deposited films will be sulfurized and then pulled off their substrate with conductive glue. The exposed surface will then be depth profiled and analyzed. Comparison with simulated depth profiles is expected to yield values for $D_b$. To generate the simulated depth profiles the software FEMLAB is being used to handle more complex geometries for the diffusion problem as well as concentration-dependent diffusion coefficients.

## *Fundamental Materials and Interface Characterization*

## Cu(InGa)$Se_2$ Optical Characterization

We have previously determined the optical constants of polycrystalline thin film $CuIn_{1-x}Ga_xSe_2$ alloys with Ga/(Ga+In) ratios from 0 to 1 using variable angle spectroscopic ellipsometry (SE) over an energy range from 0.75 to 4.6eV [1]. The films characterized in that work were all nominally single phase Cu(InGa)$Se_2$, with Cu/(In+Ga) ≈ 0.9 (or 24 at. % Cu). Subsequently, we have focused on the effect of Cu stoichiometry in Cu-poor materials on the optical properties. For the Cu-In-Se system, the $CuSe_2$-$In_2Se_3$ quasi-binary phase diagram determined by Gödecke et. al. [2] over the region of interest is shown in Figure 2. There are single phase regions containing the stoichiometric $CuInSe_2$ ($\chi$) phase and the $\delta$ phase which includes the $CuIn_3Se_5$ composition. High efficiency devices are made using films in the $\chi$ or mixed phase $\chi$+$\delta$ regions. The objective in this study is to determine how the optical functions vary, particularly in the $\chi$+$\delta$ region and across the very wide single phase $\delta$ region, and whether the behavior in the mixed phase region could be accurately fit as a mixture of the single phase constants with the relative volume fractions determined by the fit.

Cu(InGa)$Se_2$ thin films, deposited on soda lime glass/Mo substrates, with Ga/(In+Ga) = 0.3 were used for this initial study. Their Cu concentrations varied from 10 to 25 at.%, as shown in Figure 2, corresponding to Cu/(In+Ga) from 0.3 to 0.93 and the compositions are listed in Table 1. Sample preparation and the SE measurements were the same as in [1]. It is important to note that the phase diagram in Figure 2 is only verified for the CuInSe system and there may be differences when Ga is included.

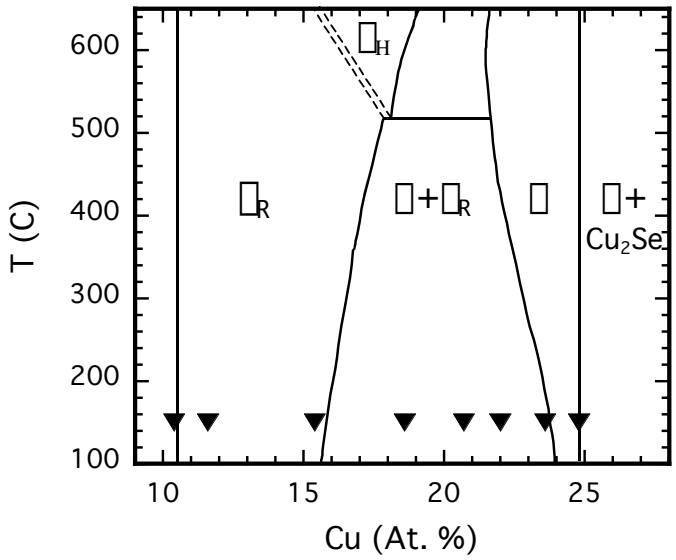


Figure 2. $Cu_2Se$-$In_2Se$ quasi-binary phase diagram taken from Reference 2. Triangles show the compositions of $Cu(InGa)Se_2$ films used in this study.

To describe the optical constants of a heterogeneous system a model is needed and 2 cases are illustrated in Figure 3. Figure 3(a) shows a coated-sphere microstructure. The dielectric response can be described by a Maxwell Garnett effective medium approximation given by the relation

$$\frac{\varepsilon - \varepsilon_a}{\varepsilon + 2\varepsilon_a} = f_b \frac{\varepsilon_b - \varepsilon_a}{\varepsilon_b + 2\varepsilon_a}$$

where $\varepsilon_a$ and $\varepsilon_b$ are, respectively, the dielectric function of the two phases a and b, $\varepsilon$ is the effective dielectric function of the heterogeneous medium, and $f_b$ is the fraction of phase b. Figure 3(b), shows a random mixture microstructure in which case the dielectric response can be described by a Bruggeman effective medium approximation given by the relation

$$0 = f_a \frac{\varepsilon_a - \varepsilon}{\varepsilon_a + 2\varepsilon} + f_b \frac{\varepsilon_b - \varepsilon}{\varepsilon_b + 2\varepsilon}.$$

Initially, the optical properties of the $Cu_x(In_{0.7}Ga_{0.3})Se_2$ alloy films were determined using multilayer optical modeling assuming the film is single phase. Based on XRD measurements, this assumption is true for $Cu(In_{0.7}Ga_{0.3})Se_2$ and $Cu(In_{0.7}Ga_{0.3})_3Se_5$ compositions. However, this assumption was later shifted and the mixed phase region was analyzed with effective medium approximations using optical constants from the end point compositions.

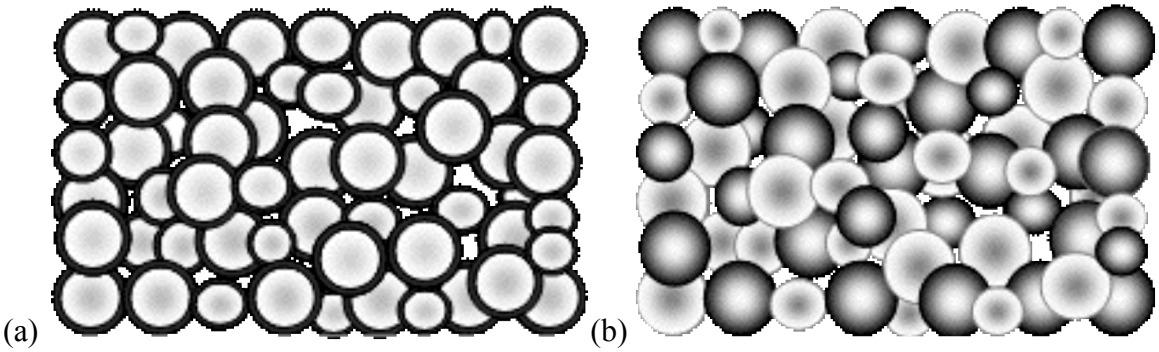

(a) (b)

Figure 3. Schematic of a coated-sphere microstructure (a) and a random mixture of 2 phases (b).

Figure 4 shows the index of refraction (n) and extinction coefficient (k) obtained from the measurements after substrate and surface roughness effects were removed using a multi-layer optical model. Samples in the mixed phase region were analyzed with effective medium approximations using optical constants from the end point compositions. Two distinctive features are visible in these optical spectra. First, the fundamental bandgaps are shifted to higher energies with decreasing Cu concentration, which can be related to the decreasing coupling between the Cu d- and Se p-orbitals, resulting in lowering of the valance band maxima. Second, the critical point features at higher energies become broader as the Cu concentration decreases. Broadening is normally associated with degradation of the crystalline quality of the material. Table 1 shows the volume fractions of the □ and □ phases using the Maxwell Garnet and Bruggeman EMA analyses. Similar results are obtained with the different models for reasons that are not clear.

$CuInSe_2$ samples with a similar distribution of Cu concentration are being prepared for similar analysis. This will allow more direct comparison with the phase diagram and more quantitative comparison of changes in the bandgap and critical energies since there will be no variation due to differences in Ga/(In+Ga).

Table 1. Compositions of $Cu(InGa)Se_2$ samples for SE analysis and the volume fraction of the a and d phases determined by the Maxwell Garnet and Bruggeman EMA analyses. MSE is the mean square error in the analysis.

| Sample | Cu | In | Ga | Se | Cu/ | Ga/ | Maxwell Garnett | | | Bruggeman | | |
|---|---|---|---|---|---|---|---|---|---|---|---|---|
| # | (%) | (%) | (%) | (%) | (In+Ga) | (In+Ga) | □ | □ | MSE | □ | □ | MSE |
| 33398 | 24.8 | 18.3 | 8.3 | 48.7 | 0.94 | 0.31 | 100 | 0 | | 100 | 0 | |
| 33579 | 23.6 | 19.9 | 7.3 | 49.2 | 0.87 | 0.27 | 100 | 0 | 10 | 100 | 0 | 9.7 |
| 33313 | 22.0 | 19.8 | 8.2 | 50.0 | 0.79 | 0.29 | 77 | 23 | 3.7 | 80 | 20 | 4.7 |
| 33538 | 20.7 | 19.6 | 9.4 | 50.3 | 0.71 | 0.32 | 52 | 48 | 2.8 | 52 | 48 | 2.8 |
| 33197 | 18.6 | 19.6 | 10.3 | 51.5 | 0.62 | 0.34 | 35 | 65 | 5.1 | 35 | 65 | 5.0 |
| 33769 | 15.4 | 22.4 | 9.7 | 52.6 | 0.48 | 0.30 | 32 | 68 | 4.1 | 32 | 68 | 4.0 |
| 33391 | 11.6 | 23.6 | 9.9 | 54.9 | 0.35 | 0.30 | 17 | 83 | 16.7 | 17 | 83 | 16.6 |
| 33786 | 10.4 | 24.2 | 11.0 | 54.4 | 0.30 | 0.31 | | | | 0 | 100 | |

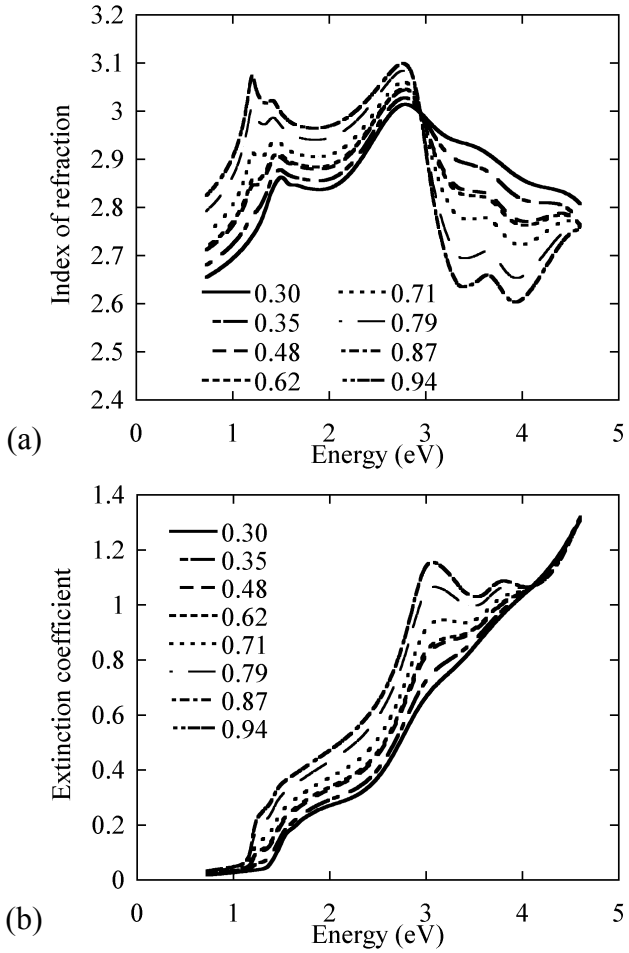


Figure 3. Optical constants of $Cu_x(In_{0.7}Ga_{0.3})Se_2$ alloy films with varying Cu concentration obtained by EMA analysis.

## Emitter Layer Deposition and Junction Characterization

Efforts have begun to study the effect of the $Cu(InGa)Se_2$/emitter layer interface and band alignment on devices by changing the alloy compositions of the $Cu(InGa)Se_2$ layers and using CdS, (CdZn)S or ZnS emitter layers. Previously we have developed CBD processes for depositing the ZnS and (CdZn)S layers. The (CdZn)S layer has bandgap 2.6 eV. These layers were deposited on $Cu(InGa)Se_2$ films with Ga/(In+Ga) = 0.3 and 0.6 eV corresponding to bandgaps of 1.2 and 1.4 eV respectively. Cell results, show that on average, the (CdZn)S gives comparable performance to the CdS emitter layer with both absorber layer bandgaps. The results for the best cell, out of 12 for each case, are summarized in Table 2. The ZnS emitter layers gave poor device efficiency in all cases and the process needs to be re-evaluated. Further experiments will expand the range of the $Cu(InGa)Se_2$ bandgap and then include more in-depth device analysis including temperature dependent J-V measurements.

Table 2. Solar cell parameters for $Cu(InGa)Se_2$ with Eg = 1.2 or 1.4 eV with CdS, (CdZn)S and ZnS emitter layers.

| Sample # | CIGS $E_g$ (eV) | Emitter layer | Eff (%) | $V_{OC}$ (V) | $J_{SC}$ (mA/cm$^2$) | FF (%) | $R_{OC}$ (Ω-cm$^2$) | $G_{SC}$ (mS/cm$^2$) |
|---|---|---|---|---|---|---|---|---|
| 50392.23 | 1.2 | CdS | 15.9 | 0.627 | 33.3 | 76.0 | 1.3 | 1 |
| 50392.33 | 1.2 | (CdZn)S | 15.7 | 0.620 | 32.7 | 77.2 | 1.3 | 2 |
| 50392.31 | 1.2 | ZnS | 10.3 | 0.547 | 31.9 | 59.1 | 2.4 | 1 |
| 50403.32 | 1.4 | CdS | 12.3 | 0.757 | 22.2 | 72.9 | 2.6 | 2 |
| 50403.21 | 1.4 | (CdZn)S | 13.9 | 0.740 | 24.9 | 75.3 | 2.1 | 1 |
| 50403.22 | 1.4 | ZnS | 4.7 | 0.613 | 18.7 | 40.5 | 10.8 | 9 |
| 50405.32 | 1.4 | CdS | 12.8 | 0.765 | 22.8 | 73.8 | 2.3 | 1 |
| 50405.21 | 1.4 | (CdZn)S | 13.0 | 0.739 | 23.8 | 73.6 | 2.3 | 1 |
| 50405.12 | 1.4 | ZnS | 6.5 | 0.594 | 23.5 | 46.4 | 5.3 | 9 |

Sincerely,

Robert W. Birkmire
Director

RWB/bj
cc: Gerri Hobbs, UD Research Office
Carolyn Lopez, NREL
Paula Newton
Erten Eser
William N. Shafarman

1. P.D. Paulson, R.W. Birkmire, W.N. Shafarman, J. Appl. Phys. **94**, 879 (2003).
2. T. Gödecke, T. Haalboom, F. Ernst, Z. Metallkd. **91**, 8 (2000).